Propagation of partially-coherent truncated polymorphic beams

MERCEDES ANGULO, JOSÉ A. RODRIGO, AND TATIANA ALIEVA*

Universidad Complutense de Madrid, Facultad de Ciencias Físicas, Ciudad Universitaria s/n, Madrid 28040, Spain

**Corresponding author: talieva@ucm.es*

Compiled April 19, 2019

The recently introduced concept of coherent polymorphic beam (PB), which is focused into a 2D light curve of arbitrary form with independently prescribed phase along it, is a fruitful generalization of the "perfect" ring vortex and opens up new perspectives in all-optical particle manipulation and light material processing. Its application for optical transport of micro/nano-particles has been experimentally demonstrated. However, the propagation of the PB has not been studied yet. In this letter, we derive analytical expressions for the propagation of the truncated PB and its partially coherent counterpart through the first-order optical systems, in particular: the rotationally symmetric and twisting systems described by the fractional Fourier and Gyrator transforms, respectively. These expressions clarify the light-curve formation from truncated PB and can be easily applied for the numerical simulation of the partially coherent PB propagation.

OCIS codes: (140.3300) Laser beam shaping; (050.4865) Optical vortices; (030.0030) Coherence and statistical optics

http://dx.doi.org/10.1364/ol.XX.XXXXXX

Laser beam shaping into a high-intensity-gradient light curve of arbitrary shape, with independently prescribed phase and polarization along it, is required in many and rather different areas: optical micro/nano-particle manipulation [1–6], light material processing at macro/micro-scale, and lithography [7, 8] to name a few. Recently we have introduced the concept of coherent polymorphic beam (PB) which, under focusing, is transformed into a 2D laser curve with desired phase and polarization along it [9, 10]. This type of beam can be seen as a fruitful generalization of the "perfect" ring vortex [11] and provides many degrees of freedom: independent control of form and size of the curve, phase and polarization distribution along the curve.

The complex field amplitude of a scalar monochromatic coherent PB is defined as [9]

$$E_{PB}\left(\mathbf{r},0\right)=\int_0^T g(t)\exp\left[-i2\pi\mu\mathbf{R}^{\mathsf{T}}\left(t\right)\mathbf{r}\right]\mathrm{d}t, \qquad (1)$$

where $\mathbf{r}=(x,y)^{\mathsf{T}}$ is a position vector in the input plane, $\mathbf{R}\left(t\right)=\left(R(t)\cos t,R(t)\sin t\right)^{\mathsf{T}}$ is a vector of the associated 2D target curve in the Fourier conjugated domain and μ is a normalization constant of dimension m^{-2}. Note that symbol $^{\mathsf{T}}$ stands for vector transposition while the italic letter $t\in[0,T]$ represented the polar angle of the parametric curve. It is easy to see that under the focusing, described by the Fourier transform (FT), the beam is transformed into the target curve $\mathbf{R}\left(t\right)$, which can be open or closed. The scale of the curve is maintained if $\mu=1/\lambda\mathrm{f}$, where λ is a wavelength and f is the focal length of the convergent lens. Note that when $\left|\mathbf{R}\left(t\right)\right|=R$ the PB is transformed, depending on $g(t)$, into the Bessel beam, which collapses under the focusing into a "perfect" ring vortex [11, 12], or into other closely related non-diffractive beams [13]. While $\mathbf{R}\left(t\right)$ describes the shape of the curve, the complex weight function [9]

$$g\left(t\right)=\left|g\left(t\right)\right|\exp\left[\mathrm{i}\frac{2\pi l}{S\left(T\right)}S\left(t\right)\right], \qquad (2)$$

controls the amplitude and phase distributions along the curve. Thus, the field amplitude distribution along the curve is given by $\left|\widetilde{E}(t)\right|=\left|g\left(t\right)\right|/\kappa\left|\dot{\mathbf{R}}(t)\right|$, where: $\left|\dot{\mathbf{R}}(t)\right|=\sqrt{\dot{R}(t)^2+R(t)^2}$ with $\dot{\mathbf{R}}(t)=\mathrm{d}\mathbf{R}(t)/\mathrm{d}t$, and $\kappa=L/\lambda\mathrm{f}$ with $L=\int_0^T\left|\dot{\mathbf{R}}(\tau)\right|\mathrm{d}\tau$ being the curve length [9]. The phase of $g(t)$, described by the real function $S(t)$, controls the phase variation along the curve and the parameter l defines the phase accumulation along the entire curve. For example, a light curve with uniform intensity distribution is obtained if $\left|g\left(t\right)\right|=E_0\kappa\left|\dot{\mathbf{R}}(t)\right|$, while $S\left(t\right)=\int_0^t\left|\dot{\mathbf{R}}(\tau)\right|\mathrm{d}\tau$ provides a uniform phase distribution along the curve $\mathbf{R}(t)$. Note that the distribution and the global accumulation (l) of the phase along the target curve do not depend on the curve shape and size.

The focused PBs have been used for optical transport of micro/nano-particles [9, 14, 15], however, the propagation of the PB, which is a goal of this letter, has not been studied yet. Moreover, here we consider the propagation of physically realizable (truncated) PBs and extend the study to the partially coherent

case. We derive analytical expressions for the propagation of Schell-model Gaussian-truncated PB through first-order optical systems [16], that allows deeper understanding of light-curve formation. In particular, we consider the propagation through rotationally symmetric and twisting systems.

First of all, similarly to Bessel-Gaussian beams [17, 18], we introduce a PB with Gaussian envelop (GPB):

$$E(\mathbf{r},0)=\exp(-\pi a|\mathbf{r}|^2)E_{PB}(\mathbf{r},0). \tag{3}$$

Here, $1/\sqrt{a}$ plays the role of the effective aperture radius required for realizable truncated PBs. Second, we assume that GPB is partially coherent (PC-GPB) and described in the input plane by its mutual intensity (MI) with a Gaussian degree of coherence $\gamma(\mathbf{r})=\exp\left(-\pi\sigma|\mathbf{r}|^2/2\right)$:

$$\begin{aligned}\Gamma(\mathbf{r}_1,\mathbf{r}_2,0) &= \exp\left(-\pi\frac{\sigma}{2}|\mathbf{r}_1-\mathbf{r}_2|^2\right)E(\mathbf{r}_1,0)E^*(\mathbf{r}_2,0)\\ &= C(\mathbf{r}_1,\mathbf{r}_2,0)E_{PB}(\mathbf{r}_1,0)E^*_{PB}(\mathbf{r}_2,0),\end{aligned} \tag{4}$$

where a and σ have dimension m^{-2}. Here, for convenience, we have introduced the MI of the partially coherent Gaussian beam $C(\mathbf{r}_1,\mathbf{r}_2,0)=\exp\left[-\pi a\left(|\mathbf{r}_1|^2+|\mathbf{r}_2|^2\right)\right]\exp\left(-\pi\frac{\sigma}{2}|\mathbf{r}_1-\mathbf{r}_2|^2\right)$.

Let us consider the propagation of the PC-GPB through a first-order optical system

$$\Gamma(\mathbf{r}_1,\mathbf{r}_2,\mathbf{H})=\iint\Gamma(\mathbf{r}_1',\mathbf{r}_2',0)K_{\mathbf{H}}(\mathbf{r}_1',\mathbf{r}_1)K^*_{\mathbf{H}}(\mathbf{r}_2',\mathbf{r}_2)\,\mathrm{d}\mathbf{r}_1'\mathrm{d}\mathbf{r}_2', \tag{5}$$

being $K_{\mathbf{H}}(\mathbf{r},\mathbf{r}')$ the kernel of the corresponding integral canonical transform (also often refereed as ABCD transform) [16]

$$K_{\mathbf{H}}(\mathbf{r}',\mathbf{r})=\frac{b^2\exp\left[i\pi b\left(\mathbf{r}^{\mathrm{T}}\mathbf{D}\mathbf{B}^{-1}\mathbf{r}-2\mathbf{r}'^{\mathrm{T}}\mathbf{B}^{-1}\mathbf{r}+\mathbf{r}'^{\mathrm{T}}\mathbf{B}^{-1}\mathbf{A}\mathbf{r}'\right)\right]}{\sqrt{\det(i\mathbf{B})}}, \tag{6}$$

which is associated with a symplectic ray transformation matrix $\mathbf{H}=\left(\begin{smallmatrix}\mathbf{A}&\mathbf{B}\\ \mathbf{C}&\mathbf{D}\end{smallmatrix}\right)$. Here $\mathbf{A}$, $\mathbf{B}$, $\mathbf{C}$ and $\mathbf{D}$ are real dimensionless 2×2 submatrices and $b=1/\lambda s$ has dimension m^{-2}. Note that $\mathbf{A}\mathbf{B}^{\mathrm{T}}=\mathbf{B}\mathbf{A}^{\mathrm{T}}$ and $\mathbf{B}^{\mathrm{T}}\mathbf{D}=\mathbf{D}^{\mathrm{T}}\mathbf{B}$ and then $\mathbf{D}\mathbf{B}^{-1}$ and $\mathbf{B}^{-1}\mathbf{A}$ are symmetric matrices. By substituting the Eqs. (1),(4),(6) in (5) and integrating over $\mathbf{r}_1$ and $\mathbf{r}_2$ using the known expression

$$\int\exp\left[-\pi\left(\mathbf{r}^{\mathrm{T}}\mathbf{P}\mathbf{r}+i2\mathbf{r}^{\mathrm{T}}\mathbf{q}\right)\right]\mathrm{d}\mathbf{r}=\frac{1}{\sqrt{\det\mathbf{P}}}\exp\left(-\pi\mathbf{q}^{\mathrm{T}}\mathbf{P}^{-1}\mathbf{q}\right) \tag{7}$$

with a 2×2 symmetric matrix $\mathbf{P}$ whose real part is positive definite, after long but straightforward calculus, we obtain the expressions for the evolution of the MI during the beam propagation through the corresponding optical systems:

$$\begin{aligned}\Gamma(\mathbf{r}_1,\mathbf{r}_2,\mathbf{H})=C(\mathbf{r}_1,\mathbf{r}_2,\mathbf{H})\cdot\tilde{\Gamma}(\mathbf{r}_1,\mathbf{r}_2,\mathbf{H})=\\ =C(\mathbf{r}_1,\mathbf{r}_2,\mathbf{H})\int_0^T\int_0^T G(t,t',\mathbf{H})\\ \times\exp\left[\pi\sigma\mu b\left(\mathbf{R}^{\mathrm{T}}(t)(\mathbf{V}\mathbf{M})^{-1}\mathbf{B}^{-1}\mathbf{r}_2+\mathbf{R}^{\mathrm{T}}(t')(\mathbf{V}\mathbf{M})^{-1}\mathbf{B}^{-1}\mathbf{r}_1\right)\right]\\ \times\exp\left[-2\pi\mu b\left(\mathbf{R}^{\mathrm{T}}(t)\left(\mathbf{V}^{-1}\right)^*\mathbf{B}^{-1}\mathbf{r}_1+\mathbf{R}^{\mathrm{T}}(t')\mathbf{V}^{-1}\mathbf{B}^{-1}\mathbf{r}_2\right)\right]\mathrm{d}t\mathrm{d}t'.\end{aligned} \tag{8}$$

Here, $C(\mathbf{r}_1,\mathbf{r}_2,\mathbf{H})$ corresponds to the propagated MI of the Gaussian partially coherent beam:

$$\begin{aligned}C(\mathbf{r}_1,\mathbf{r}_2,\mathbf{H})=\frac{b^2}{|\det\mathbf{B}|\sqrt{\det\mathbf{M}\det\mathbf{V}}}\\ \times\exp\left[-\pi b\mathbf{r}_1^{\mathrm{T}}\left[b(\mathbf{B}^{-1})^{\mathrm{T}}\left(\mathbf{V}^{-1}\right)^*\mathbf{B}^{-1}-\mathrm{i}\mathbf{D}\mathbf{B}^{-1}\right]\mathbf{r}_1\right]\\ \times\exp\left[-\pi b\mathbf{r}_2^{\mathrm{T}}\left[b(\mathbf{B}^{-1})^{\mathrm{T}}\mathbf{V}^{-1}\mathbf{B}^{-1}+\mathrm{i}\mathbf{D}\mathbf{B}^{-1}\right]\mathbf{r}_2\right]\\ \times\exp\left[\pi\sigma b^2\mathbf{r}_1^{\mathrm{T}}\left(\mathbf{B}^{-1}\right)^{\mathrm{T}}(\mathbf{V}\mathbf{M})^{-1}\mathbf{B}^{-1}\mathbf{r}_2\right],\end{aligned} \tag{9}$$

and

$$\begin{aligned}G(t,t',\mathbf{H})=G(t,t',0)\exp\left[\pi\sigma\mu^2\mathbf{R}^{\mathrm{T}}(t)(\mathbf{V}\mathbf{M})^{-1}\mathbf{R}(t')\right]\\ \times\exp\left[-\pi\mu^2\left(\mathbf{R}^{\mathrm{T}}(t)\left(\mathbf{V}^{-1}\right)^*\mathbf{R}(t)+\mathbf{R}^{\mathrm{T}}(t')\mathbf{V}^{-1}\mathbf{R}(t')\right)\right],\end{aligned} \tag{10}$$

where

$$\begin{aligned}\mathbf{M}=-ib\mathbf{B}^{-1}\mathbf{A}+\mathbf{I}(\sigma/2+a)=\mathbf{M}^{\mathrm{T}},\\ \mathbf{V}=\mathbf{M}^*-\sigma^2\mathbf{M}^{-1}/4=\mathbf{V}^{\mathrm{T}},\\ (\mathbf{V}\mathbf{M})^{-1}=\left[(\mathbf{M}^*\mathbf{M}-\sigma^2\mathbf{I}/4)\right]^{-1}=\left[(\mathbf{V}\mathbf{M})^{-1}\right]^*\end{aligned} \tag{11}$$

with $\mathbf{I}$ being a 2×2 unity matrix, and $G(t,t',0)=g(t)g^*(t')$. The Eqs. (8)-(10) allow analyzing the PC-GPB propagation through any first-order optical system with $\det\mathbf{B}\neq0$. We observe that the MI of the PC-GPB at any plane of the system, including the input one, is given as the product of the MI of the corresponding partially coherent Gaussian beam and the MI of the beam $\tilde{\Gamma}(\mathbf{r}_1,\mathbf{r}_2,\mathbf{H})$ related to the PB characteristics: curve equation $\mathbf{R}(t)$, input weight function $g(t)$, normalization constant μ as well as the parameters a and σ associated with the input Gaussian envelop and the input coherence degree, respectively.

For more detailed analysis, we take into account the modified Iwasawa decomposition [19] and the cascadability of the canonical transform. Then, we consider the evolution of the MI, $\Gamma(\mathbf{r}_1,\mathbf{r}_2|\,\mathbf{U})$, only in the systems related to the phase-space rotations described by the 2×2 unitary matrix $\mathbf{U}=\mathbf{X}+\mathrm{i}\mathbf{Y}=\mathbf{S}^{-1}(\mathbf{A}+\mathrm{i}\mathbf{B})$. Indeed, $\Gamma(\mathbf{r}_1,\mathbf{r}_2|\,\mathbf{H})$ can be easily obtained from $\Gamma(\mathbf{r}_1,\mathbf{r}_2|\,\mathbf{U})$ by applying the corresponding scaling and phase modulation

$$\begin{aligned}\Gamma(\mathbf{r}_1,\mathbf{r}_2|\,\mathbf{H}) &= |\det(\mathbf{S})|^{-1}\exp\left[-\mathrm{i}\pi\left(\mathbf{r}_1^{\mathrm{T}}\mathbf{G}\mathbf{r}_1-\mathbf{r}_2^{\mathrm{T}}\mathbf{G}\mathbf{r}_2\right)\right]\\ &\times\ \Gamma(\mathbf{S}^{-1}\mathbf{r}_1,\mathbf{S}^{-1}\mathbf{r}_2|\,\mathbf{U}),\end{aligned} \tag{12}$$

where $\mathbf{S}=\left(\mathbf{A}\mathbf{A}^{\mathrm{T}}+\mathbf{B}\mathbf{B}^{\mathrm{T}}\right)^{1/2}$ and $\mathbf{G}=-\left(\mathbf{C}\mathbf{A}^{\mathrm{T}}+\mathbf{D}\mathbf{B}^{\mathrm{T}}\right)\mathbf{S}^{-2}$.

There are two important phase-space rotators [19]: Symmetric fractional Fourier transform (frFT), $\mathbf{U}_f^{\alpha}=\exp(\mathrm{i}\alpha)\mathbf{I}$, and gyrator transform, $\mathbf{U}_g^{\alpha}=\cos\alpha\mathbf{I}+\mathrm{i}\sin\alpha\mathbf{J}$, associated with the beam propagation through rotationally symmetric and twisting optical systems, respectively. Here, we have introduced the matrix $\mathbf{J}=\left(\begin{smallmatrix}0&1\\1&0\end{smallmatrix}\right)$. In these cases, the matrices in the Eq. (6) are simplified. For the frFT $\mathbf{B}=\sin\alpha\mathbf{I}$, $\mathbf{D}\mathbf{B}^{-1}=\mathbf{B}^{-1}\mathbf{A}=\cot\alpha\mathbf{I}$, while for the gyrator transform $\mathbf{B}=\sin\alpha\mathbf{J}$ and $\mathbf{M}=-ib\cot\alpha\mathbf{J}+(\sigma+a)\mathbf{I}$. The final expression for the MI propagation, one of the main

results of this paper, is given by

$$\Gamma(\mathbf{r}_1,\mathbf{r}_2,\mathbf{U}^{\alpha}_{f,g}) = C(\mathbf{r}_1,\mathbf{r}_2,\mathbf{U}^{\alpha}_{f,g}) \int_0^T\int_0^T G(t,t',\mathbf{U}^{\alpha}_{f,g}) \times \exp\left[-\mathrm{i}\frac{2\pi\mu b^2\cos\alpha}{w^2}\left(\mathbf{R}^{\mathrm{T}}(t)\,\mathbf{r}_1 - \mathbf{R}^{\mathrm{T}}(t')\,\mathbf{r}_2\right)\right] \times \exp\left[-\frac{\pi\sigma\mu b\sin\alpha}{w^2}\left(\mathbf{R}^{\mathrm{T}}(t) - \mathbf{R}^{\mathrm{T}}(t')\right)\mathbf{\Lambda}(\mathbf{r}_1-\mathbf{r}_2)\right] \times \exp\left[-\frac{2\pi a\mu b\sin\alpha}{w^2}\left(\mathbf{R}^{\mathrm{T}}(t)\,\mathbf{\Lambda}\mathbf{r}_1 + \mathbf{R}^{\mathrm{T}}(t')\,\mathbf{\Lambda}\mathbf{r}_2\right)\right]\mathrm{d}t\mathrm{d}t' \quad (13)$$

where $w^2 = b^2\cos^2\alpha + a(\sigma+a)\sin^2\alpha$,

$$C(\mathbf{r}_1,\mathbf{r}_2,\mathbf{U}^{\alpha}_{f,g}) = \frac{b^2}{w^2}\exp\left[-\pi\frac{2\sigma b^2}{w^2}|\mathbf{r}_1-\mathbf{r}_2|^2\right] \times \exp\left[-\pi\frac{ab^2}{w^2}\left(|\mathbf{r}_1|^2+|\mathbf{r}_2|^2\right)\right] \times \exp\left[-\mathrm{i}\pi\frac{b\left(b^2-a(\sigma+a)\right)\sin 2\alpha}{2w^2}\left[\mathbf{r}_1{}^{\mathrm{T}}\mathbf{\Lambda}\mathbf{r}_1 - \mathbf{r}_2{}^{\mathrm{T}}\mathbf{\Lambda}\mathbf{r}_2\right]\right] \quad (14)$$

and

$$G(t,t',\mathbf{U}^{\alpha}_{f,g}) = G(t,t',0)\exp\left(-\frac{\pi\sigma\mu^2\sin^2\alpha}{2w^2}|\mathbf{R}(t)-\mathbf{R}(t')|^2\right) \times \exp\left[-\frac{\pi a\mu^2\sin^2\alpha}{w^2}\left(|\mathbf{R}(t)|^2+|\mathbf{R}(t')|^2\right)\right] \times \exp\left[-\mathrm{i}\frac{\pi b\mu^2\sin 2\alpha}{2w^2}\left(\mathbf{R}^{\mathrm{T}}(t)\,\mathbf{\Lambda}\mathbf{R}(t) - \mathbf{R}^{\mathrm{T}}(t')\,\mathbf{\Lambda}\mathbf{R}(t')\right)\right]. \quad (15)$$

Here $\mathbf{\Lambda} = \mathbf{I}$ and $\mathbf{\Lambda} = \mathbf{J}$ for the case of the frFT and gyrator transform, correspondingly. We observe that the main difference between these two cases is the form of the "smoothing" terms (see the two last real-valued exponential terms in Eq. (13)) related to Gaussian truncation and partial coherence. In particular, this will be the only difference for Fourier plane $\alpha = \pi/2$. It is easy to prove that for $\alpha = 0$ the Eq. (13) is reduced to the Eq. (4) and for a and σ tending to 0 and $\alpha = \pi/2$ the beam is transformed into the tight light curve. The evolution of the weight function $G(t,t',\mathbf{U}^{\alpha}_{f,g})$ is described by similar exponential terms as there are in $C(\mathbf{r}_1,\mathbf{r}_2,\mathbf{U}^{\alpha}_{f,g})$, see Eq. (15), but with $\mathbf{R}(t)$ and $\mathbf{R}(t')$ instead of $\mathbf{r}_1$ and $\mathbf{r}_2$. In the PC-GPB case, the integrals over t and t' are not separable anymore due to the second exponential in $G(t,t',\mathbf{U}^{\alpha}_{f,g})$ even for the calculus of the intensity distribution $I(\mathbf{r},\mathbf{U}^{\alpha}_{f,g}) = \Gamma(\mathbf{r},\mathbf{r},\mathbf{U}^{\alpha}_{f,g})$ derived from Eq. (13) by the simple substitution $\mathbf{r}_1 = \mathbf{r}_2 = \mathbf{r}$.

As an example, we consider propagation through rotationally symmetric systems, associated with the frFT, that includes a free space propagation for $\alpha \in [0,\pi/2]$. Since theoretical and experimental analysis of the MI, which is a 4D complex function, is difficult, then the easily measurable intensity distribution $I(\mathbf{r},\mathbf{U}^{\alpha}_{f}) = \Gamma(\mathbf{r},\mathbf{r},\mathbf{U}^{\alpha}_{f})$ and 2D cross-correlation function (CCF), $\mathrm{CCF}(\mathbf{r},\mathbf{U}^{\alpha}_{f}) = \Gamma(\mathbf{r},-\mathbf{r},\mathbf{U}^{\alpha}_{f})$ [20, 21] are often used instead, for beam characterization. The evolution of the intensity distribution and the CCF during beam propagation are described by the

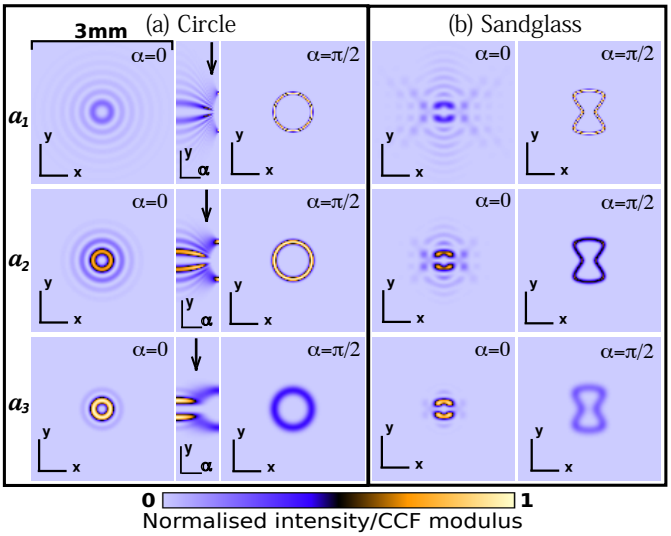

Fig. 1. Evolution of the $I(\mathbf{r},\mathbf{U}^{\alpha}_{f}) = \left|\mathrm{CCF}(\mathbf{r},\mathbf{U}^{\alpha}_{f})\right|$ during the propagation of the ring-GPB (a) and sandglass-GPB (b). The $1/\sqrt{a}$ takes three values: $7R_0$ (first row), $7R_0/2$ (second row), and $7R_0/4$ (third row). The first and the last columns in (a) and (b) correspond to input ($\alpha = 0$) and Fourier ($\alpha = \pi/2$) planes. The second column in (a) displays the evolution of the distribution profile for the ring-GPB during the beam propagation $\alpha \in [0,\pi/2]$, whereas Visualization 1 shows the evolution for the sandglass-GPB. The angle α_c is marked with a down arrow.

following equations:

$$I(\mathbf{r},\mathbf{U}^{\alpha}_{f}) = \frac{b^2}{w^2}\exp\left(-\frac{2\pi b^2 a}{w^2}|\mathbf{r}|^2\right)\int_0^T\int_0^T G(t,t',\mathbf{U}^{\alpha}_{f}) \times \exp\left[-\mathrm{i}\frac{2\pi\mu b^2\cos\alpha}{w^2}\left(\mathbf{R}^{\mathrm{T}}(t) - \mathbf{R}^{\mathrm{T}}(t')\right)\mathbf{r}\right] \times \exp\left[-\frac{2\pi\mu ba\sin\alpha}{w^2}\left(\mathbf{R}^{\mathrm{T}}(t) + \mathbf{R}^{\mathrm{T}}(t')\right)\mathbf{r}\right]\mathrm{d}t\mathrm{d}t' \quad (16)$$

and

$$\mathrm{CCF}(\mathbf{r},\mathbf{U}^{\alpha}_{f}) = \frac{b^2}{w^2}\exp\left[-\frac{2\pi b^2(a+\sigma)}{w^2}|\mathbf{r}|^2\right]\int_0^T\int_0^T G(t,t',\mathbf{U}^{\alpha}_{f}) \times \exp\left[-\mathrm{i}\frac{2\pi\mu b^2\cos\alpha}{w^2}\left(\mathbf{R}^{\mathrm{T}}(t) + \mathbf{R}^{\mathrm{T}}(t')\right)\mathbf{r}\right] \times \exp\left[-\frac{2\pi\mu b(\sigma+a)\sin\alpha}{w^2}\left(\mathbf{R}^{\mathrm{T}}(t) - \mathbf{R}^{\mathrm{T}}(t')\right)\mathbf{r}\right]\mathrm{d}t\mathrm{d}t', \quad (17)$$

where

$$G(t,t',\mathbf{U}^{\alpha}_{f}) = G(t,t',0)\exp\left(-\frac{\pi\sigma\mu^2\sin^2\alpha}{2w^2}|\mathbf{R}(t)-\mathbf{R}(t')|^2\right) \times \exp\left[-\frac{\pi a\mu^2\sin^2\alpha}{w^2}\left(|\mathbf{R}(t)|^2+|\mathbf{R}(t')|^2\right)\right] \times \exp\left[-\mathrm{i}\frac{\pi b\mu^2\sin 2\alpha}{2w^2}\left(|\mathbf{R}(t)|^2 - |\mathbf{R}(t')|^2\right)\right]. \quad (18)$$

Figures 1 and 2 present the propagation of the intensity and CCF modulus distributions for two PC-GPBs, one associated with a ring target curve, the helical Bessel beam

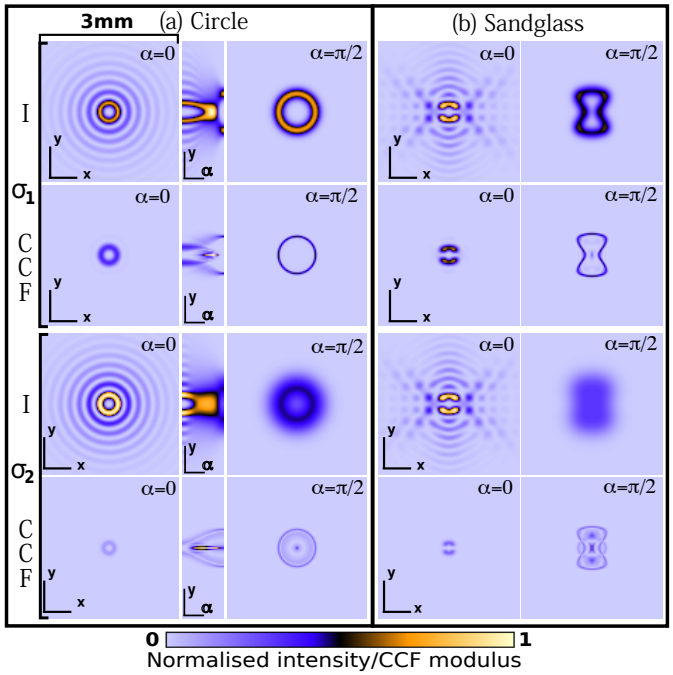

Fig. 2. Evolution of the $I(\mathbf{r},\mathbf{U}_f^{\alpha})$ and $\left|\mathrm{CCF}(\mathbf{r},\mathbf{U}_f^{\alpha})\right|$ during the propagation of the ring-PC-GPB (a) and sandglass-PC-GPB (b). The transversal coherence length takes the values $1/\sqrt{\sigma_1} = 7R_0/5$ (first two rows), $1/\sqrt{\sigma_2} = 7R_0/10$ (second two rows). The first and the last columns in (a) and (b) correspond to input ($\alpha = 0$) and Fourier ($\alpha = \pi/2$) planes. The second column in (a) displays the evolution of the distributions profiles for the ring-PC-GPB during the beam propagation $\alpha \in [0, \pi/2]$, whereas Visualization 2 shows the evolution for the sandglass-PC-GPB.

(ring-GPB), $R(t) = R_0 = 1/\sqrt{\mu} = 0.4$ mm and the other, with a sandglass one given (sandglass-GPB) by $R(t) = R_0\left[|1.1\cos(t)|^{17} + |0.1\sin(t)|^{\frac{3}{2}}\right]^{\frac{-1}{4\cdot 2}}$, both with uniform amplitude and phase distributions ($l = 2$). By having chosen the parameters $\lambda = 532$ nm, $\mathrm{f} = \mathrm{s} = 300$ mm, then $\mu = b = 6.3 \cdot 10^6 \mathrm{m}^{-2}$ and these curves are described by $R(t)$ without any scaling in Fourier plane. For a proper propagation analysis, the $I(\mathbf{r},\mathbf{U}_f^{\alpha})$ and $\left|\mathrm{CCF}(\mathbf{r},\mathbf{U}_f^{\alpha})\right|$ have been normalized to the maximum value of the entire set ($\alpha \in [0, \pi/2]$) in every studied case (given a and σ).

Fig. 1 shows the case of fully coherent light ($\sigma = 0$) for three different values of a. Due to point symmetry of the considered curves $\mathbf{R}(\mathbf{r}) = \mathbf{R}(-\mathbf{r})$ when $\sigma = 0$ the intensity distribution equals to the modulus of the CCF. The first and last columns in Fig. 1(a) and Fig. 1(b) display the $I(\mathbf{r},\mathbf{U}_f^{\alpha}) = \left|\mathrm{CCF}(\mathbf{r},\mathbf{U}_f^{\alpha})\right|$ in the input ($\alpha = 0$) and Fourier ($\alpha = \pi/2$) planes, correspondingly. We observe that the decrease of the effective aperture $1/\sqrt{a}$ yields to a shape blurring of the target curve, as expected. Moreover, analysing the evolution of the intensity profiles for the ring-GPB (Fig. 1(a), middle column) we observe that the value of the α_c, where the formation of the target curve starts, decreases for smaller effective apertures. Interesting phenomenon occurs when the form of the curve is different from the circle. We have found that the intensity distribution for sandglass-GPB is "axis asymmetric" for $\alpha \neq n\pi/2$, with integer n, and makes a flip when the sign of l is changed, in spite of the rotationally symmetry of the system (see $x-y$ intensity distribution evolution for sandglass curve, Visualisation 1).

Fig. 2 present the evolution of the $I(\mathbf{r},\mathbf{U}_f^{\alpha})$ and $\left|\mathrm{CCF}(\mathbf{r},\mathbf{U}_f^{\alpha})\right|$ for ring and sandglass PC-GPBs with effective aperture $1/\sqrt{a} = 7R_0$. Note that, even for symmetric curves, $I(\mathbf{r},\mathbf{U}_f^{\alpha}) \neq \left|\mathrm{CCF}(\mathbf{r},\mathbf{U}_f^{\alpha})\right|$ in the partially coherent case ($\sigma \neq 0$). We observe that the decrease of the coherence also produces the blurring of the intensity distribution of the target light curves up to their transformation to almost uniform intensity distribution with slightly notable curve contour. However, in spite of the curve information washing in the intensity distribution in the Fourier plane, the $\left|\mathrm{CCF}(\mathbf{r},\mathbf{U}_f^{\alpha})\right|$ maintains a well-defined fine structure for $\alpha = \pi/2$ which correlates with the curve shape even for relatively low coherence length $1/\sqrt{\sigma} = 0.1/\sqrt{a}$ (see second and forth rows of Fig. 2(a) and (b)). These findings illustrate the importance of the beam coherence characteristics which have longer "memory" of the beam structure than the intensity distribution, as observed in the last columns of Fig. 2.

Finally, we conclude that the derived expression for the MI evolution of the PC-GPB during propagation through a general first-order optical system (see Eq. (8-10)) and its reduced version for two principal phase-space rotators: fractional FT and gyrator (see Eq. (13-15)) are an important start point for the analytical and numerical study of the PC-GPB. The experimental study of the PC-GPBs can be performed with the system reported in [22].

FUNDING

The *Ministerio de Economía y Competitividad* is acknowledged for funding the project TEC2014-57394-P. This research was partially supported through a Santander-UCM project (PR75/18-21567).

REFERENCES

1. H. He, M. E. J. Friese, N. R. Heckenberg, and H. Rubinsztein-Dunlop, Phys. Rev. Lett. **75**, 826 (1995).
2. K. T. Gahagan and G. a. Swartzlander, Opt. Lett. **21**, 827 (1996).
3. J. Arlt, V. Garces-Chavez, W. Sibbett, and K. Dholakia, Opt. Commun. **197**, 239 (2001).
4. S.-h. S. Lee, Y. Roichman, and D. D. G. Grier, Opt. Express **18**, 1974 (2010).
5. E. R. Shanblatt and D. G. Grier, Opt. Express **19**, 5833 (2011).
6. J. A. Rodrigo and T. Alieva, Optica **2**, 812 (2015).
7. M. Duocastella and C. Arnold, Laser Photon. Rev. **6**, 607 (2012).
8. J. Hamazaki, R. Morita, K. Chujo, Y. Kobayashi, S. Tanda, and T. Omatsu, Opt. Express **18**, 2144 (2010).
9. J. A. Rodrigo and T. Alieva, Sci. Reports **6**, 35341 (2016).
10. J. A. Rodrigo and T. Alieva, Sci. Reports **8**, 7698 (2018).
11. P. Vaity and L. Rusch, Opt. Lett. **40**, 597 (2015).
12. Y. Roichman and D. G. Grier, Proc. SPIE **10003**, 64830F (2007).
13. J. Durnin, J. Opt. Soc. Am. A **4**, 651 (1987).
14. J. A. Rodrigo and T. Alieva, Sci. Rep. **6**, 33729 (2016).
15. J. A. Rodrigo, M. Angulo, and T. Alieva, Opt. Lett. **43**, 4244 (2018).
16. J. J. Healy, M. A. Kutay, H. M. Ozaktas, and J. T. Sheridan, *Linear Canonical Transforms.Theory and Applications* (Springer, NY, 2015).
17. F. Gori, G. Guattari, and C. Padovani, Opt. Commun. **64**, 491 (1987).
18. J. Turunen and A. T. Friberg, Prog. Opt. **54**, 1 (Elsevier, 2010).
19. R. Simon and K. B. Wolf, J. Opt. Soc. Am. A **17**, 342 (2000).
20. D. M. Palacios, I. D. Maleev, a. S. Marathay, and G. a. Swartzlander, Phys. Rev. Lett. **92**, 143905 (2004).
21. Y. Yang, M. Chen, M. Mazilu, A. Mourka, Y.-D. Liu, and K. Dholakia, New J. Phys. **15**, 113053 (2013).
22. T. Alieva, J. A. Rodrigo, A. Cámara, and E. Abramochkin, J. Opt. Soc. Am. A **30**, 2237 (2013).

REFERENCES

1. H. He, M. E. J. Friese, N. R. Heckenberg, and H. Rubinsztein-Dunlop, "Direct Observation of Transfer of Angular Momentum to Absorptive Particles from a Laser Beam with a Phase Singularity," Phys. Rev. Lett. **75**, 826–829 (1995).
2. K. T. Gahagan and G. a. Swartzlander, "Optical vortex trapping of particles." Opt. Lett. **21**, 827–9 (1996).
3. J. Arlt, V. Garces-Chavez, W. Sibbett, and K. Dholakia, "Optical micromanipulation using a Bessel light beam," Optics Communications **197**, 239 – 245 (2001).
4. S.-h. S. Lee, Y. Roichman, and D. D. G. Grier, "Optical solenoid beams," Opt. Express **18**, 1974–1977 (2010).
5. E. R. Shanblatt and D. G. Grier, "Extended and knotted optical traps in three dimensions." Opt. Express **19**, 5833–5838 (2011).
6. J. A. Rodrigo and T. Alieva, "Freestyle 3D laser traps: tools for studying light-driven particle dynamics and beyond," Optica **2**, 812–815 (2015).
7. M. Duocastella and C. Arnold, "Bessel and annular beams for materials processing," Laser Photon. Rev. **6**, 607–621 (2012).
8. J. Hamazaki, R. Morita, K. Chujo, Y. Kobayashi, S. Tanda, and T. Omatsu, "Optical-vortex laser ablation," Opt. Express **18**, 2144–2151 (2010).
9. J. A. Rodrigo and T. Alieva, "Polymorphic beams and Nature inspired circuits for optical current," Scientific Reports **6**, 35341 (2016).
10. J. A. Rodrigo and T. Alieva, "Vector polymorphic beam," Scientific Reports **8**, 7698 (2018).
11. P. Vaity and L. Rusch, "Perfect vortex beam: Fourier transformation of a Bessel beam." Opt. Lett. **40**, 597–600 (2015).
12. Y. Roichman and D. G. Grier, "Three-dimensional holographic ring traps," Proc. SPIE **10003**, 64830F–64830F–5 (2007).
13. J. Durnin, "Exact solutions for nondiffracting beams. I. The scalar theory," J. Opt. Soc. Am. A **4**, 651 (1987).
14. J. A. Rodrigo and T. Alieva, "Light-driven transport of plasmonic nanoparticles on demand," Sci. Rep. **6**, 33729 (2016).
15. J. A. Rodrigo, M. Angulo, and T. Alieva, "Programmable optical transport of particles in knot circuits and networks," Opt. Lett. **43**, 4244–4247 (2018).
16. J. J. Healy, M. A. Kutay, H. M. Ozaktas, and J. T. Sheridan, *Linear Canonical Transforms.Theory and Applications* (Springer, NY, 2015).
17. F. Gori, G. Guattari, and C. Padovani, "Bessel-Gauss beams," Optics Communications **64**, 491 – 495 (1987).
18. J. Turunen and A. T. Friberg, "Propagation-Invariant Optical Fields," Progress in Optics **54**, 1–88 (Elsevier, 2010).
19. R. Simon and K. B. Wolf, "Structure of the set of paraxial optical systems," J. Opt. Soc. Am. A **17**, 342–355 (2000).
20. D. M. Palacios, I. D. Maleev, a. S. Marathay, and G. a. Swartzlander, "Spatial Correlation Singularity of a Vortex Field," Phys. Rev. Lett. **92**, 143905 (2004).
21. Y. Yang, M. Chen, M. Mazilu, A. Mourka, Y.-D. Liu, and K. Dholakia, "Effect of the radial and azimuthal mode indices of a partially coherent vortex field upon a spatial correlation singularity," New J. Phys. **15**, 113053 (2013).
22. T. Alieva, J. A. Rodrigo, A. Cámara, and E. Abramochkin, "Partially coherent stable and spiral beams," J. Opt. Soc. Am. A **30**, 2237–2243 (2013).